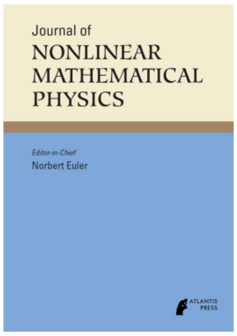

ATLANTIS PRESS

Journal of Nonlinear Mathematical Physics

ISSN (Online): 1776-0852 **ISSN (Print): 1402-9251**
Journal Home Page: https://www.atlantis-press.com/journals/jnmp

Final evolutions of a class of May-Leonard Lotka-Volterra systems

Claudio A. Buzzi, Robson A. T. Santos, Jaume Llibre

To cite this article: Claudio A. Buzzi, Robson A. T. Santos, Jaume Llibre (2020) Final evolutions of a class of May-Leonard Lotka-Volterra systems, Journal of Nonlinear Mathematical Physics 27:2, 267–278, DOI: https://doi.org/10.1080/14029251.2020.1700635

To link to this article: https://doi.org/10.1080/14029251.2020.1700635

Published online: 04 January 2021

Journal of Nonlinear Mathematical Physics, Vol. 27, No. 2 (2020) 267–278

Final evolutions of a class of May-Leonard Lotka-Volterra systems

Claudio A. Buzzi and Robson A. T. Santos

Departamento de Matemática, Universidade Estadual Paulista,
Rua Cristóvão Colombo 2265, São José do Rio Preto, 15115-000, Brazil
claudio.buzzi@unesp.br and robson.trevizan@outlook.com

Jaume Llibre

Departament de Matemàtiques, Universitat Autònoma de Barcelona,
Edificio C Facultad de Ciencias, Bellaterra (Barcelona), Catalonia, 08193, Spain
jllibre@mat.uab.cat

Received 8 June 2019

Accepted 29 August 2019

We study a particular class of Lotka-Volterra 3-dimensional systems called May-Leonard systems, which depend on two real parameters a and b, when $a+b=-1$. For these values of the parameters we shall describe its global dynamics in the compactification of the non-negative octant of $\mathbb{R}^3$ including its infinity. This can be done because this differential system possesses a Darboux invariant.

Keywords: May-Leonard system; Lotka-Volterra system; invariant, global dynamics.

2000 Mathematics Subject Classification: 34D45, 34D05, 37N25, 92D25, 34C12

1. Introduction

Polynomial ordinary differential systems are often used in various branches of applied mathematics, physics, chemist, engineering, etc. Models studying the interaction between species of predator-prey type have been extensively analyzed as the classical Lotka-Volterra systems. For more information on the Lotka-Volterra systems see for instance [8] and the references quoted there. In particular, one of these competition models between three species inside the class of 3-dimensional Lotka-Volterra systems is the *May-Leonard model* given by the polynomial differential system in $\mathbb{R}^3$

$$\begin{aligned} \dot{x} &= x(1-x-ay-bz),\\ \dot{y} &= y(1-bx-y-az),\\ \dot{z} &= z(1-ax-by-z), \end{aligned} \tag{1.1}$$

where a and b are real parameters and the dot denotes derivative with respect to the time t. See for more details on the May-Leonard system the papers [10] and [2] and on Lotka-Volterra systems [9], and the references quoted there.

The Lotka-Volterra systems in $\mathbb{R}^3$ have the property that the three coordinate planes are invariant by the flow of these systems. Moreover, at points of straight line $x=y=z$, system (1.1) is reduced to $\dot{x}=x-(1+a+b)x^2$, because the other equations do not provide any further information. Therefore, the bisectrix of the non-negative octant is an invariant straight line for this differential system.

In this paper we describe the global dynamics of system (1.1) in function of the parameters a and b when $a+b=-1$. The system (1.1) is defined in $\mathbb{R}^3$. In order to study the dynamics of its orbits at infinity we extend analytically its flow by using the Poincaré compactification of $\mathbb{R}^3$. In the appendix we give precise definitions for this compactification. The region of interest in our study is the non-negative octant of $\mathbb{R}^3$, i.e. where $x \geq 0, y \geq 0, z \geq 0$. So we shall study the flow of the Poincaré compactification in the region

$$R = \{(x,y,z) \in \mathbb{R}^3 : x^2+y^2+z^2 \leq 1, x \geq 0, y \geq 0, z \geq 0\}$$

of the Poincaré ball.

We remark that the global dynamics of the May-Leonard system (1.1) with $a+b=-1$ can be studied because this differential system has a Darboux invariant.

The differential system (1.1) has been extensively studied in order to understand the interaction between species and try to predict possible extinction or overpopulation for example. However our interest is purely mathematical, we want to illustrate how the Darboux invariant can be used to describe the global dynamics of a differential system. Note that we are interested in the study of system (1.1) for all real values of the parameters a and b satisfying $a+b=-1$, and not only for their positive values. Consequently our analysis has no biological meaning. This study could be made in a similar way in the others octants of $\mathbb{R}^3$.

2. Statement of the main results

We denote by X the polynomial vector field associated to the differential system (1.1), and by $p(X)$ the Poincaré compactification of X, see the appendix in section 5. The flow of system (1.1) in the region R is described in the next two theorems. For a formal definition of topologically equivalent phase portraits see [5].

Theorem 2.1. *For the May-Leonard differential system* (1.1) *in the octant R the following statements hold when* $a+b=-1$.

(a) *The phase portrait of the Poincaré compactification* $p(X)$ *of system* (1.1) *on the boundaries* $x=0$, $y=0$ *and* $z=0$ *of R is topologically equivalent to the one described in Fig.* 1(a) *if* $a \leq -2$ *or* $a \geq 1$, *and in Fig.* 2(a) *if* $-2 < a < 1$.

(b) *The phase portrait of the Poincaré compactification* $p(X)$ *of system* (1.1) *on* $R^\infty = \partial R \cap \{x^2+y^2+z^2=1\}$ (*i.e. the phase portrait at the infinity of the non-negative octant of* $\mathbb{R}^3$) *is topologically equivalent to the one described in Fig.* 1(b) *if* $a \leq -2$ *or* $a \geq 1$, *Fig.* 2(b) *if* $a=-1/2$, *Fig.* 2(c) *if* $-2 < a < -1/2$, *and Fig.* 2(d) *if* $-1/2 < a < 1$. *In particular, there are no periodic orbits in* R^∞.

(c) *When* $a=-1/2$ *the planes* $x=y$, $x=z$ *and* $y=z$ *are invariant by the flow of system* (1.1), *and the phase portrait of the Poincaré compactification* $p(X)$ *of system* (1.1) *on* $R \cap \{x=y\}$, $R \cap \{x=z\}$ *and* $R \cap \{y=z\}$ *are topologically equivalent to the ones described in* (a), (b) *and* (c) *of Fig.* 3 *respectively.*

Let $p(\gamma)$ denote the orbit γ of the vector field X associated to system (1.1) in the Poincaré compactification $p(X)$.

Theorem 2.2. *Let* γ *be an orbit of system* (1.1) *with* $a+b=-1$ *such that* $p(\gamma)$ *is contained in the interior of R. Then the following statements hold.*

(a) *If $a \leq -2$ or $a \geq 1$ then we have:*

(i) *The α-limit set of $p(\gamma)$ is either the origin of $\mathbb{R}^3$, or the heteroclinic loop connecting the singular points p_1, p_2 and p_3, or the heteroclinic loop connecting the singular points p_x^∞, p_y^∞ and p_z^∞ (see Fig.* 1(a)).

(ii) *The ω-limit set of $p(\gamma)$ is either p_b^∞ (the positive endpoint of the bisectrix $x = y = z$), or the heteroclinic loop connecting the singular points p_x^∞, p_y^∞ and p_z^∞ (see Figure* 1(b)).

(b) *If $-2 < a < 1$ then we have:*

(i) *The α-limit set of $p(\gamma)$ is one of the singular points p_j for $j = 0, 1 \ldots, 6$ or p_x^∞, p_y^∞, p_z^∞, p_{xy}^∞, p_{xz}^∞, p_{yz}^∞ (see Fig.* 2(a)).

(ii) *The ω-limit set of $p(\gamma)$ is p_b^∞, the positive endpoint of the bisectrix $x = y = z$ (see Figure* 2(b)(c)(d)).

An immediate consequence of Theorem 2.2 is the following result.

Corollary 2.1. *All orbit γ of system* (1.1) *with $a+b = -1$ such that $p(\gamma)$ is contained in the interior of R has their α-limit in $xyz = 0$ and their ω-limit in R^∞.*

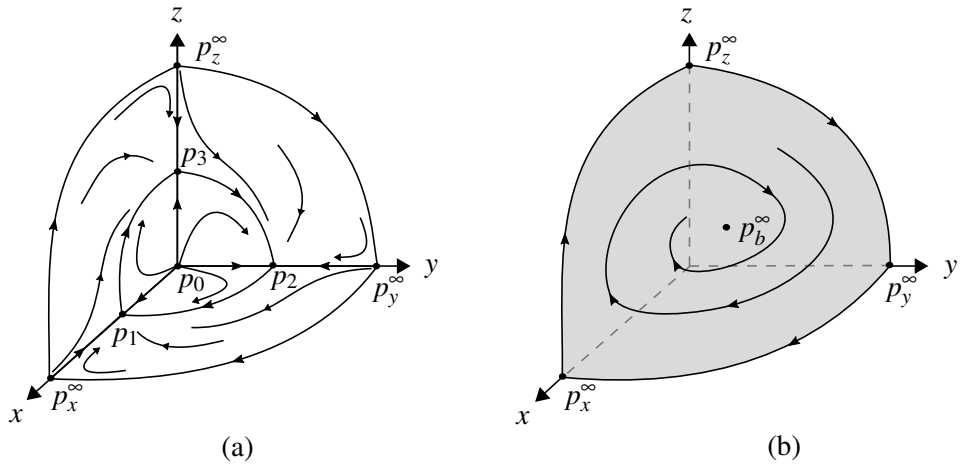

Fig. 1. The global dynamics on the boundary of R for $a+b = -1$ and $a \leq -2$. (a) The dynamics on $xyz = 0$. (b) The dynamics on R^∞. Reversing the sense of all the orbits we have the global dynamics on the boundary of R for $a+b = -1$ and $a \geq 1$.

3. Proof of Theorem 1

The following two lemmas will be useful to the proof of Theorem 1.

Lemma 3.1. *The May-Leonard differential system* (1.1) *with $a+b = -1$ has four finite equilibrium points in the case $a \leq -2$ or $a \geq 1$, and has seven finite equilibrium points in the case $-2 < a < 1$. Moreover, the local dynamics around these equilibrium points are presented in Figures* 1(a) *and* 2(a).

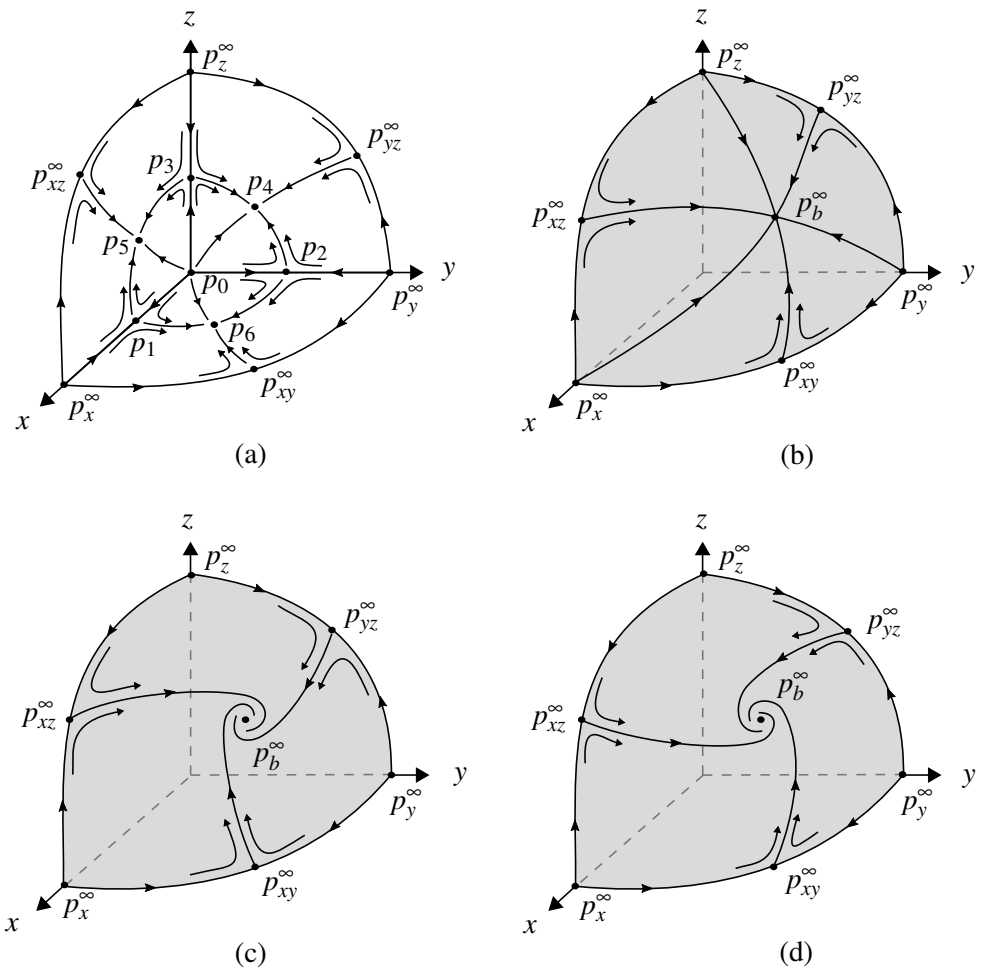

Fig. 2. The global dynamics on the boundary of R for $a+b=-1$ and $-2<a<1$. (a) The dynamics on $xyz=0$. The dynamics on R^∞ for $a=-1/2$ in (b), for $a\in(-2,-1/2)$ in (c), and for $a\in(-1/2,1)$ in (d).

Proof. The finite singular points of system (1.1) with $a+b=-1$ are the solutions of the system

$$\begin{aligned} P_1(x,y,z) &= x(1-x+z+a(-y+z))=0,\\ P_2(x,y,z) &= y(1+x-y+a(-z+x))=0,\\ P_3(x,y,z) &= z(1+y-z+a(-x+y))=0, \end{aligned}$$

namely

$$p_0=(0,0,0),\quad p_1=(1,0,0),\quad p_2=(0,1,0),\quad p_3=(0,0,1),$$

$$p_4=\left(0,\frac{1-a}{A},\frac{2+a}{A}\right),\quad p_5=\left(\frac{2+a}{A},0,\frac{1-a}{A}\right),\quad p_6=\left(\frac{1-a}{A},\frac{2+a}{A},0\right),$$

where $A=1+a+a^2$.

Since $A>0$ for $a\in\mathbb{R}$ and the region of interest is R, we have:

(i) If $a\le -2$ or $a\ge 1$ system (1.1) has only four finite equilibrium points: p_0, p_1, p_2 and p_3.

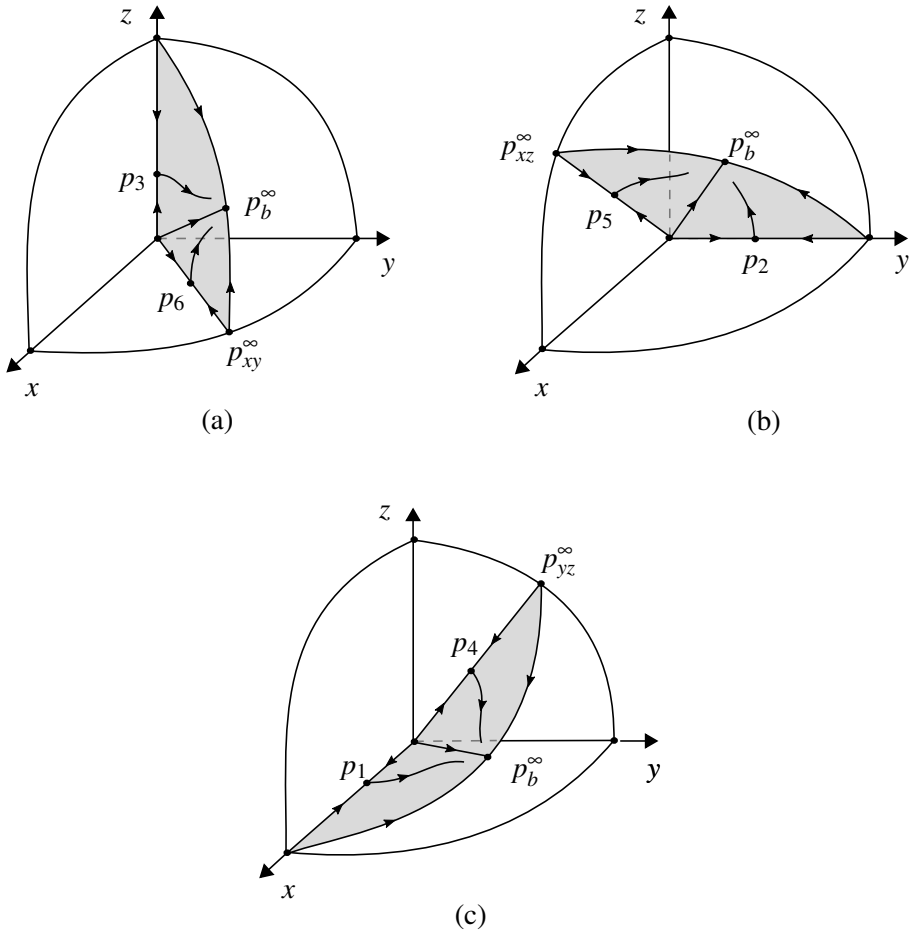

Fig. 3. The global dynamics on $R \cap \{x = y\}$, $R \cap \{x = z\}$ and $R \cap \{y = z\}$ respectively, when $a = b = -1/2$.

(ii) If $-2 < a < 1$ system (1.1) has the seven finite equilibrium points p_j for $j = 0, 1 \ldots, 6$.

All these finite equilibrium points are hyperbolic if $a \neq -2, 1$, and consequently its local phase portrait is topologically equivalent to the phase portrait of its linear part by the Hartman–Grobman Theorem, see for instance [4].

We note that when $a \in (-2, 1)$ and $a \to 1$ we have that $p_4 \to p_3$, $p_5 \to p_1$ and $p_6 \to p_2$; while if $a \to -2$ we have that $p_4 \to p_2$, $p_5 \to p_3$ and $p_6 \to p_1$. This behavior of these equilibria allows to determine by continuity the local phase portraits on the boundary of R of the non-hyperbolic equilibrium points p_1, p_2 and p_3 when $a = -2$ and $a = 1$ from the global phase portraits of the boundary of R when $a \in (-2, 1)$.

The linear part of system (1.1) at the equilibrium p_0 is the identity matrix. Therefore it is a repelling equilibrium.

The eigenvalues of linear part at equilibrium points p_1, p_2 and p_3 are -1, $1-a$, $2+a$. Therefore when $a < -2$ or $a > 1$ these equilibria have a 2-dimensional stable manifold and an 1-dimensional unstable one; and for $-2 < a < 1$ these equilibria have a 2-dimensional unstable manifold and an 1-dimensional stable one.

When $-2<a<1$ the eigenvalues of linear part at equilibrium points p_4, p_5 and p_6 are 3, -1 and $(-2+a+a^2)/A$. Since $-2+a+a^2<0$ for $-2<a<1$ then these equilibria have a 2-dimensional stable manifold and an 1-dimensional unstable one. Moreover, p_4 (respectively p_5 and p_6) is an attractor restricted to the invariant boundary $x=0$ (respectively $y=0$ and $z=0$). Now we explain in few words, what we mean by saying that the local phase portraits, for $a=-2$ and $a=1$, can be determined by continuity. For example, if $a\in(-2,1)$ then, on the plane $x=0$, we have that p_4 is a node and p_2 is a saddle. If a tends to -2 then p_4 tends to p_2 and we have a saddle-node bifurcation. For $a=-2$ we have that $p_4=p_2$ is a saddle-node singularity with two hyperbolic sectors in the half-plane $\{x=0,y<0\}$ and a parabolic sector in the half-plane $\{x=0,y>0\}$. So, in a neighborhood of p_2 contained in the half-plane $\{x=0,y>0\}$, the local phase portraits are the same for $a=-2$ or $a<-2$ in the non-negative octant. The same analysis can be done for the other points p_1 and p_3, and for the case when a tends to 1. □

Lemma 3.2. *The May-Leonard differential system* (1.1) *with* $a+b=-1$ *has four infinite equilibrium points in the case* $a\le -2$ *or* $a\ge 1$*, and has seven infinite equilibrium points in the case* $-2<a<1$*. Moreover, the local dynamics around these equilibrium points are presented in Figures* 1(b), 2(b), 2(c) *and* 2(d).

Proof. Now we shall study the infinite equilibrium points. For study the dynamics on the infinity R^∞ of R we shall use the Poincaré compactification of the differential system (1.1). See appendix for details. Thus the differential system (1.1) in the local chart U_1 becomes

$$\begin{aligned}\dot{z_1}&=2z_1+az_1-z_1^2+az_1^2-z_1z_2-2az_1z_2,\\ \dot{z_2}&=z_2-az_2+z_1z_2+2az_1z_2-2z_2^2-az_2^2,\\ \dot{z_3}&=z_3+az_1z_3-z_2z_3-az_2z_3-z_3^2.\end{aligned}\tag{3.1}$$

So system (1.1), with $a+b=-1$ and satisfying $a\le -2$ or $a\ge 1$, has two equilibrium points at infinity: $(0,0,0)$ and $(1,1,0)$. We call the first one p_x^∞ the positive endpoint of the x-axis, and the second one p_b^∞ the positive endpoint of the bisectrix $x=y=z$. The linear part at the equilibrium p_x^∞ has the eigenvalues $1-a$ and $2+a$ at infinity and eigenvalue 1 in its finite direction. Therefore, on the infinity p_x^∞ is a saddle such that its stable separatrix is contained in the z_1-axis when $a\le -2$ (respectively z_2-axis when $a\ge 1$).

The eigenvalues of linear part at equilibrium p_b^∞ are $(-3\pm i\sqrt{3}(1+2a))/2$ and 0. Therefore, on the infinity p_b^∞ is a stable focus turning clockwise if $a\le -2$ (respectively counterclockwise if $a\ge 1$).

Now system (1.1) in the local chart U_2 writes

$$\begin{aligned}\dot{z_1}&=z_1-az_1-2z_1^2-az_1^2+z_1z_2+2az_1z_2,\\ \dot{z_2}&=2z_2+az_2-z_1z_2-2az_1z_2-z_2^2+az_2^2,\\ \dot{z_3}&=z_3-z_1z_3-az_1z_3+az_2z_3-z_3^2.\end{aligned}\tag{3.2}$$

Since the local chart U_2 covers the end part of the plane $x=0$ at infinity of the non-negative octant of $\mathbb{R}^3$, we are interested only in the equilibrium points which are on $z_1=0$ and $z_3=0$. In this case, with $a+b=-1$ and satisfying $a\le -2$ or $a\ge 1$, there is one equilibrium point at infinity: $(0,0,0)$. We call this equilibrium p_y^∞ the positive endpoint of the y-axis. The eigenvalues of linear part at equilibrium p_y^∞ are $1-a$ and $2+a$ at infinity and eigenvalue 1 in its finite direction. Therefore, on

the infinity p_y^∞ is a saddle such that its stable separatrix is contained in the z_2-axis when $a \leq -2$ (respectively z_1-axis when $a \geq 1$).

Now for $a \leq -2$ or $a \geq 1$ we only need to study the equilibrium point at the endpoint of positive z-half-axis, i.e. the equilibrium point at the origin of the local chart U_3. We call this equilibrium point p_z^∞. In the local chart U_3 system (1.1) becomes

$$\begin{aligned}
\dot{z_1} &= 2z_1 + az_1 - z_1^2 + az_1^2 - z_1z_2 - 2az_1z_2,\\
\dot{z_2} &= z_2 - az_2 + z_1z_2 + 2az_1z_2 - 2z_2^2 - az_2^2,\\
\dot{z_3} &= z_3 + az_1z_3 - z_2z_3 - az_2z_3 - z_3^2.
\end{aligned}$$

The linear part at the equilibrium point p_z^∞ has eigenvalues $1-a$ and $2+a$ at infinity and eigenvalue 1 in its finite direction. Therefore the origin of the local chart U_3 is a saddle such that its stable separatrix is contained in the z_1-axis when $a \leq -2$ (respectively z_2-axis when $a \geq 1$).

We have proved that the phase portrait of system (1.1) on R^∞, for $a+b=-1$ and $a \leq -2$, is the one presented in Figure $1(b)$. In the same figure, reversing the sense of all the orbits, we have the global dynamics on R^∞, for $a+b=-1$ and $a \geq 1$.

It remains to study the infinite equilibrium points of system (1.1) in case $-2 < a < 1$. In the local chart U_1 the system (3.1) has four equilibrium points at infinity: $p_x^\infty = (0,0,0)$, $p_{xy}^\infty = ((2+a)/(1-a),0,0)$, $p_{xz}^\infty = (0,(1-a)/(2+a),0)$ and $p_b^\infty = (1,1,0)$. The eigenvalues of linear part at equilibrium p_x^∞ are $1-a$ and $2+a$ at infinity and eigenvalue 1 in its finite direction. Then this equilibrium is an unstable node. The linear part at the equilibrium p_{xy}^∞ (respectively p_{xz}^∞) has the eigenvalues $-(2+a)$, $A/(1-a)$ and $3A/(1-a)$ (respectively $(a-1)$, $A/(2+a)$ and $3A/(2+a)$). Therefore the equilibria p_{xy}^∞ and p_{xz}^∞ are saddles such that their stable separatrix is contained in the z_1-axis and z_2-axis respectively. The eigenvalues of the linear part at the equilibrium p_b^∞ are $(-3 \pm i\sqrt{3}(1+2a))/2$ and 0. Therefore, on the infinity p_b^∞ is a stable focus turning clockwise if $-2 < a < -1/2$ (respectively counterclockwise if $-1/2 < a < 1$). When $a = -1/2$ on the infinity p_b^∞ is stable node.

Now since we are interested only in the equilibrium points which are on $z_1 = 0$ and $z_3 = 0$, in the local chart U_2 the system (3.2) has two equilibrium points: $p_y^\infty = (0,0,0)$ and $p_{yz}^\infty = (0,(2+a)/(1-a),0)$. The eigenvalues of linear part at equilibrium p_y^∞ are $1-a$ and $2+a$ at infinity and eigenvalue 1 in its finite direction. Then, on the infinity this equilibrium is an unstable node. The linear part at the equilibrium $(0,(2+a)/(1-a),0)$ has the eigenvalues $-(2+a)$, $A/(1-a)$ and $3A/(1-a)$ at infinity. Therefore, on the infinity $p_{yz}^\infty = (0,(2+a)/(1-a),0)$ is a saddle such that its stable separatrix is contained in the z_2-axis.

In the local chart U_3 we only need to study the equilibrium point $p_z^\infty = (0,0,0)$. The eigenvalues of linear part at this equilibrium are $1-a$ and $2+a$ at infinity and eigenvalue 1 in its finite direction. Then, on the infinity this equilibrium is an unstable node.

We conclude that the infinite equilibrium points of system (1.1) with$a+b=-1$ in case $-2<a<1$ are

p_x^∞ = the positive endpoint of the x-axis,
p_y^∞ = the positive endpoint of the y-axis,
p_z^∞ = the positive endpoint of the z-axis,
p_{xz}^∞ = the positive endpoint of the straight line $(a-1)x+(2+a)z=0$, $y=0$,
p_{xy}^∞ = the positive endpoint of the straight line $(2+a)x+(a-1)y=0$, $z=0$,
p_{yz}^∞ = the positive endpoint of the straight line $(2+a)y+(a-1)z=0$, $x=0$,
p_b^∞ = the positive endpoint of the bisectrix $x=y=z$,

and the phase portraits of system (1.1) on R^∞, for $a+b=-1$ and $-2<a<1$, are presented in Figures $2(b)$, $2(c)$ and $2(d)$.

We also observe that when $a\in(-2,1)$ and $a\to 1$ we have that $p_{xz}^\infty\to p_x^\infty$, $p_{yz}^\infty\to p_z^\infty$, and $p_{xy}^\infty\to p_y^\infty$; while if $a\to -2$ we have that $p_{xz}^\infty\to p_z^\infty$, $p_{yz}^\infty\to p_y^\infty$, and $p_{xy}^\infty\to p_x^\infty$. So the behavior of these equilibria allows to determine by continuity the local phase portraits on the boundary of R of the non-hyperbolic equilibrium which are at the positive endpoints of the axes of coordinates when $a=-2$ and $a=1$ from the global phase portraits of the boundary of R when $a\in(-2,1)$. □

We will show now that does not exist a periodic orbit on R^∞. For this we will need Bautin's Theorem, which is proved in [1].

Theorem 3.1 (Bautin's Theorem). *A quadratic polynomial differential system of the form*

$$\dot{x}=x(a_0+a_1x+a_2y),\quad \dot{y}=x(b_0+b_1x+b_2y),$$

has no limit cycles.

Lemma 3.3. *There are no periodic orbits of the Poincaré compactification of the vector field associated to system* (1.1) *in the Poincaré compactification on* R^∞.

Proof. The differential system (1.1) in the local chart U_1 is given by (3.1). Making $z_3=0$ to determine the dynamics on R^∞ we have the system

$$\begin{aligned}\dot{z_1}&=z_1\big((2+a)+(a-1)z_1-(1+2a)z_2\big),\\ \dot{z_2}&=z_2\big((1-a)+(1+2a)z_1-(2+a)z_2\big).\end{aligned}\tag{3.3}$$

By Bautin's Theorem, the system (3.3) has no limit cycles. In addition, system (3.3) has only two equilibrium points: $(z_1,z_2)=(0,0)$ and $(z_1,z_2)=(1,1)$. The linear part at the equilibrium $(0,0)$ has the eigenvalues $1-a$ and $2+a$, and the eigenvalues of linear part at equilibrium $(1,1)$ are $(-3\pm i\sqrt{3}(1+2a))/2$. Therefore, both $(0,0)$ and $(1,1)$ are not centers. Thus, the only possibility of periodic orbit in R^∞ would be to have a limit cycle, which we have already seen is not possible. □

So, using Lemmas 3.1, 3.2 and 3.3, the proof of statements (a) and (b) of Theorem 2.1 is complete.

Now since the bisectrix $x=y=z$ is an invariant straight line for the system, it is easy to check for $a=-1/2$ that the global phase portrait on the invariant planes $R\cap\{x=y\}$, $R\cap\{x=z\}$ and $R\cap\{y=z\}$ are topologically equivalents to the ones described in (a), (b) and (c) of Fig. 3 respectively. This completes the proof of Theorem 2.1.

4. Proof of Theorem 2

We say that a C^1 function $I(x,y,z,t)$ is an *invariant* of the polynomial differential system (1.1) if $I(x(t),y(t),z(t),t)$ is constant, for all the values of t for which the solution $(x(t),y(t),z(t))$ of (1.1) is defined. When the function I is independent of the time, then it is called a *first integral* of differential system (1.1). Also if an invariant $I(x,y,z,t)$ is of the form $f(x,y,z)e^{st}$, then it is called a *Darboux invariant*.

Proposition 4.1. *System* (1.1)*, for* $a+b=-1$*, has the Darboux invariant* $I = I(t,x,y,z) = xyze^{-3t}$.

Proof. It is immediate to check that

$$\frac{dI}{dt} = \frac{\partial I}{\partial x}\dot{x} + \frac{\partial I}{\partial y}\dot{y} + \frac{\partial I}{\partial z}\dot{z} + \frac{\partial I}{\partial t} = 0,$$

where $\dot{x}$, $\dot{y}$ and $\dot{z}$ are given in (1.1). Therefore I is a Darboux invariant of system (1.1). □

For knowing how to obtain the Darboux invariant given in Proposition 4.1 see statement (vi) of Theorem 8.7 of [5], there the theory is described for polynomial vector fields in $\mathbb{R}^2$, but the results and the proofs extend to $\mathbb{R}^3$.

Proposition 4.2. *Let* $I(x,y,z,t) = f(x,y,z)e^{st}$ *be a Darboux invariant of system* (1.1)*. Let* $p \in \mathbb{R}^3$ *and* $\varphi_p(t)$ *the solution of system* (1.1) *such that* $\varphi_p(0) = p$*. Then*

$$\alpha(p), \omega(p) \subset \overline{\{f(x,y,z) = 0\} \cup \mathbb{S}^2}.$$

Here $\alpha(p)$ *and* $\omega(p)$ *denote the* α*-limit and* ω*-limit sets of* p *respectively, and* $\mathbb{S}^2$ *denotes the boundary of the Poincaré ball, i.e. the infinity of* $\mathbb{R}^3$.

For a proof of Proposition 4.2 see [7].

Lemma 4.1. *Let* $p(\gamma) = \{\varphi_p(t) = (x(t),y(t),z(t)) : t \in \mathbb{R}\}$ *be the orbit of the Poincaré compactification of system* (1.1)*, for* $a+b=-1$*, such that* $\varphi_p(0) = p$ *and* $\lim_{t\to+\infty} x(t)y(t)z(t) = +\infty$*. Then* $\omega(p) \subset R^\infty$.

Proof. Let $q \in \omega(p)$. Then there exists a sequence (t_n) with $t_n \to +\infty$, such that $\varphi_p(t_n) = (x(t_n),y(t_n),z(t_n)) \to q$ when $n \to +\infty$. By Proposition 4.2 we know that $q \in \{(x,y,z) \in R : xyz = 0\} \cup R^\infty$. Suppose that $q \notin R^\infty$ and take $\varepsilon > 0$. Then there exist $M > 0$ and $n_0 \in \mathbb{N}$ such that $xyz \le M$ for all $x,y,z \in \overline{B(q,\varepsilon)}$ and $\varphi_p(t_n) \in \overline{B(q,\varepsilon)}$ for all $n \ge n_0$. Therefore $x(t_n)y(t_n)z(t_n) \le M$ for all $n \ge n_0$. On the other hand, as $\lim_{t\to+\infty} x(t)y(t)z(t) = +\infty$ then exists $t_0 \in \mathbb{R}$ such that $x(t)y(t)z(t) \ge M$ for all $t \ge t_0$, which is a contradiction. Therefore $q \in R^\infty$. □

Proof. [Proof of Theorem 2.2] Let $p(\gamma) = \{\varphi_p(t) = (x(t),y(t),z(t)) : t \in \mathbb{R}\}$ be the orbit of the Poincaré compactification of system (1.1) with $a+b=-1$ such that $\varphi_p(0) = p$ with p in the interior of R. We recall that all the orbits of a differential system defined on a compact set are defined for all $t \in \mathbb{R}$. By Propositions 4.1 and 4.2 the α- and ω-limit set of $p(\gamma)$ is contained in boundary of R, i.e. in $\{(x,y,z) \in R : xyz = 0\} \cup R^\infty$. Furthermore, by Proposition 4.1, $I(t,x(t),y(t),z(t)) = k$ constant

with $k > 0$. So

$$x(t)y(t)z(t) = ke^{3t}, \tag{4.1}$$

for all t. Taking limit in (4.1) when $t \to -\infty$, we obtain

$$\lim_{t\to-\infty} x(t)y(t)z(t) = 0.$$

This implies that the orbit $p(\gamma)$ tends to the set $xyz = 0$ when $t \to -\infty$. Looking at the dynamics of the flow of the compactified vector field on $xyz = 0$ described in Fig. 1(a) if $a \leq -2$ or $a \geq 1$, and in Fig. 2(a) if $-2 < a < 1$, we consider the following two cases.

Case 1. Suppose that $a \leq -2$ or $a \geq 1$. Therefore, by Theorem 2.1(a) and Fig. 1(a) we have that the α-limit set of $p(\gamma)$ can be the equilibrium point p_0 because the eigenvalue at p_0 is 1 with multiplicity three. The equilibrium points p_1, p_2, p_3, p_x^∞, p_y^∞ and p_z^∞ can not be α-limit set of $p(\gamma)$ in the case that $p(\gamma)$ is a characteristic orbit, because the unstable separatrix of the saddles are contained in the faces of R. But other possible sets to be α-limit of the orbit $p(\gamma)$ in the interior of R is either the heteroclinic loop connecting the equilibrium points p_1, p_2 and p_3, or the heteroclinic loop connecting the equilibrium points p_x^∞, p_y^∞ and p_z^∞. So statement (a)(i) of Theorem 2.2 is proved.

Case 2. Assume that $-2 < a < 1$. By Theorem 2.1(a) and Fig. 2(a) we have that the singular points p_0, p_x^∞, p_y^∞ and p_z^∞ are repelling. Furthermore, the singular points p_j for $j = 1,2,\ldots,6$ and p_{xy}^∞, p_{xz}^∞, p_{yz}^∞ are of saddle type such that their 2-dimensional unstable manifold intersect the interior of R. Therefore, the α-limit set of $p(\gamma)$ can be one of the singular points p_j for $j = 0,1\ldots,6$ or p_x^∞, p_y^∞, p_z^∞, p_{xy}^∞, p_{xz}^∞, p_{yz}^∞. So statement (b)(i) of Theorem 2.2 is proved.

Now we study the ω-limit set of $p(\gamma)$. In a similar way taking limit in (4.1) when $t \to +\infty$ we obtain

$$\lim_{t\to+\infty} x(t)y(t)z(t) = +\infty.$$

So by Proposition 4.2 and by Lemma 4.1 we conclude that the ω-limit set of $p(\gamma)$ is contained in R^∞. Looking at the dynamics of the flow of the compactified vector field on R^∞ described in Fig. 1(b) if $a \leq -2$ or $a \geq 1$, we conclude that the ω-limit set of $p(\gamma)$ is the infinite singular point $p_b^\infty \in R^\infty$ or the heteroclinic loop connecting the singular points p_x^∞, p_y^∞ and p_z^∞. So, the proof of statement (a)(ii) of Theorem 2.2 is complete. Furthermore, if $-2 < a < 1$, looking in Figs. 2(b)(c)(d) we conclude that the ω-limit set of $p(\gamma)$ is the infinite singular point $p_b^\infty \in R^\infty$. Hence statement (b)(ii) of Theorem 2.2 is proved. □

Remark 4.1. An interesting question is: Can we say something for other values of the parameters a and b? As we have mentioned at the beginning of Section 4, both *Darboux invariant* and *first integral* are *invariants* to the system (1.1). Leach and Miritzis [6] obtained the following first integrals:

(i) $H_1 = \frac{xyz}{(x+y+z)^3}$ if $a+b = 2$ and $a \neq 1$,
(ii) $H_2 = \frac{y(x-z)}{x(y-z)}$ if $a = b \neq 1$,
(iii) $H_3 = \frac{x}{z}$ and $H_4 = \frac{y}{z}$ if $a = b = 1$.

The global dynamics in these cases was studied in [2].

Appendix

A. The Poincaré compactification in $\mathbb{R}^3$

For more details on the Poincaré compactification in $\mathbb{R}^3$ see [3]. In $\mathbb{R}^3$ we consider the polynomial differential system

$$\dot{x} = P_1(x,y,z), \quad \dot{y} = P_2(x,y,z), \quad \dot{z} = P_3(x,y,z),$$

or equivalently its associated polynomial vector field $X = (P_1, P_2, P_3)$. The degree n of X is defined as $n = \max\{\deg(P_i) : i = 1,2,3\}$.

Let $\mathbb{S}^3 = \{y = (y_1, y_2, y_3, y_4) \in \mathbb{R}^4 : \|y\| = 1\}$ be the unit sphere in $\mathbb{R}^4$, and

$$\mathbb{H}_+ = \{y \in \mathbb{S}^3 : y_4 > 0\} \quad \text{and} \quad \mathbb{H}_- = \{y \in \mathbb{S}^3 : y_4 < 0\}$$

be the northern and southern hemispheres, respectively. The tangent space to $\mathbb{S}^3$ at the point y is denoted by $T_y\mathbb{S}^3$. Then we identify the tangent hyperplane

$$T_{(0,0,0,1)}\mathbb{S}^3 = \{(x_1, x_2, x_3, 1) \in \mathbb{R}^4 : (x_1, x_2, x_3) \in \mathbb{R}^3\}$$

with $\mathbb{R}^3$.

We consider the central projections

$$f_+ : \mathbb{R}^3 = T_{(0,0,0,1)}\mathbb{S}^3 \to \mathbb{H}_+ \quad \text{and} \quad f_- : \mathbb{R}^3 = T_{(0,0,0,1)}\mathbb{S}^3 \to \mathbb{H}_-,$$

defined by

$$f_+(x) = \frac{1}{\Delta x}(x_1, x_2, x_3, 1) \quad \text{and} \quad f_-(x) = -\frac{1}{\Delta x}(x_1, x_2, x_3, 1),$$

where $\Delta x = (1 + \sum_{i=1}^3 x_i^2)^{1/2}$. Through these central projection $\mathbb{R}^3$ is identified with the northern and the southern hemispheres, respectively. The equator of the sphere $\mathbb{S}^3$ is $\mathbb{S}^2 = \{y \in \mathbb{S}^3 : y_4 = 0\}$. Clearly $\mathbb{S}^2$ can be identified with the *infinity* of $\mathbb{R}^3$.

The diffeomorphisms f_+ and f_- define two copies of X, one $Df_+ \circ X$ in the northern hemisphere and the other $Df_- \circ X$ in the southern one. Denote by $\bar{X}$ the vector field on $\mathbb{S}^3 \setminus \mathbb{S}^2 = \mathbb{H}_+ \cup \mathbb{H}_-$ such that restricted to $\mathbb{H}_+$ coincides with $Df_+ \circ X$ and restricted to $\mathbb{H}_-$ coincides with $Df_- \circ X$. We extend analytically the polynomial vector field $\bar{X}$ to the equator of $\mathbb{S}^3$, i.e. to the infinity of $\mathbb{R}^3$, in such a way that the flow on the boundary is invariant. This is done defining the vector field

$$p(X)(y) = y_4^{n-1}\bar{X}(y),$$

for all $y \in \mathbb{S}^3$. This extended vector field $p(X)$ is called the *Poincaré compactification of* X on the Poincaré sphere $\mathbb{S}^3$.

In what follows we shall work with the orthogonal projection of the closed northern hemisphere to $y_4 = 0$. Note that this projection is a closed ball B of radius one, whose interior is diffeomorphic to $\mathbb{R}^3$ and whose boundary $\mathbb{S}^2$ corresponds to the infinity of $\mathbb{R}^3$. The projected vector field on B is called the *Poincaré compactification* on the Poincaré ball B.

As $\mathbb{S}^3$ is a differentiable manifold, to compute the expression for $p(X)$ we can consider the eight local charts (U_i, F_i), (V_i, G_i) where $U_i = \{y \in \mathbb{S}^3 : y_i > 0\}$ and $V_i = \{y \in \mathbb{S}^3 : y_i < 0\}$ for $i = 1,2,3,4$; the diffeomorphisms $F_i : U_i \to \mathbb{R}^3$ and $G_i : V_i \to \mathbb{R}^3$ for $i = 1,2,3,4$, are the inverses of the central

projections from the origin to the tangent planes at the points $(\pm 1,0,0,0)$, $(0,\pm 1,0,0)$, $(0,0,\pm 1,0)$ and $(0,0,0,\pm 1)$, respectively. The expression of $p(X)$ on the local chart U_1 is

$$z_3^n(-z_1P_1+P_2,-z_2P_1+P_3,-z_3P_1), \tag{A.1}$$

where $P_i = P_i(1/z_3, z_1/z_3, z_2/z_3)$, and the expressions of $p(X)$ in U_2 is

$$z_3^n(-z_1P_2+P_1,-z_2P_2+P_3,-z_3P_2), \tag{A.2}$$

where $P_i = P_i(z_1/z_3, 1/z_3, z_2/z_3)$ in U_2, and in U_3 is

$$\frac{z_3^n}{(\Delta z)^{n-1}}(-z_1P_3+P_1,-z_2P_3+P_2,-z_3P_3), \tag{A.3}$$

where $P_i = P_i(z_1/z_3, z_2/z_3, 1/z_3)$ in U_3.

The expression for $p(X)$ in U_4 is $z_3^{n+1}(P_1,P_2,P_3)$ where the component $P_i = P_i(z_1,z_2,z_3)$. The expression for $p(X)$ in the local chart V_i is the same as in U_i multiplied by $(-1)^{n-1}$. We remark that all the points on the sphere at infinity in the coordinates of any local chart have $z_3 = 0$.

Acknowledgments

The first author is supported by FAPESP grant 2013/2454-1 and CAPES grant 88881.068462/2014-01. The second author is partially supported by the Ministerio de Economía, Industria y Competitividad, Agencia Estatal de Investigación grant MTM2016-77278-P (FEDER), the Agència de Gestió d'Ajuts Universitaris i de Recerca grant 2017SGR1617, and the H2020 European Research Council grant MSCA-RISE-2017-777911. The third author is supported by CAPES grant 99999.006888/2015-01 from the program CAPES-PDSE.

References

[1] N.N. Bautin, On the number of limit cycles which appear with the variation of coefficients from an equilibrium position of focus or center type (R), *Mat. Sb.*, **30** (72) (1952), 181–196; *Amer. Math. Soc. Trans. No.*, **100** (1954).

[2] G. Blé, V. Castellanos, J. Llibre, I. Quilantán, Integrability and global dynamics of the May-Leonard model, *Nonlinear Anal.*, **14** (2013), 280–293.

[3] A. Cima and J. Llibre, Bounded polynomial vector fields, *Trans. Amer. Math. Soc.*, **318** (1990), 557–579.

[4] P. Hartman, A lemma in the theory of structural stability of differential equations, *Proc. Amer. Math. Soc.*, **11**, 610–620.

[5] F. Dumortier, J. Llibre and J.C. Artés, *Qualitative Theory of Planar Differential Systems*, (Universitext Springer, New York, 2006).

[6] P.G.L. Leach, J. Miritzis, Analytic behaviour of competition among three species, *J. Nonlinear Math. Phys.*, **13** (2006), 535-?548.

[7] J. Llibre and R.D.S. Oliveira, Quadratic systems with invariant straight lines of total multiplicity two having Darboux invariants, *Communications in Contemporary Mathematics*, **17** (2015), 145001, pp 17.

[8] J. Llibre and C. Valls, Polynomial, rational and analytic first integrals for a family of 3-dimensional Lotka-Volterra systems, *Z. Angew. Math. Phys.*, **62** (2011), 761–777.

[9] J. Llibre and C. Valls, Proper rational and analytic first integrals for asymmetric 3-dimensional Lotka-Volterra systems, *J. Nonlinear Math. Phys.*, **24** (2017), 393–404.

[10] R.M. May and W.J. Leonard, Nonlinear aspects of competition between three species, *SIAM J. Appl. Math.*, **29** (1975), 243–253.